BMC Chemistry

RESEARCH ARTICLE

Open Access

Enhanced room temperature gas sensing properties of low temperature solution processed ZnO/CuO heterojunction

P. P. Subha and M. K. Jayaraj*

Abstract

The development of room temperature gas sensors having response towards a specific gas is attracting researchers nowadays in the field. In the present work, room temperature (29 °C) ethanol sensor based on vertically aligned ZnO nanorods decorated with CuO nanoparticles was successfully fabricated by simple cost effective solution processing. The heterojunction sensor exhibits better sensor parameters compared to pristine ZnO. The response of the heterojunction sensor to 50 ppm ethanol is, at least, 2-fold higher than the response of the ZnO bare sensor. Also the response and recovery time of ZnO/CuO sensor to 50 ppm ethanol are of 9 and 420 s whereas the values are 16 and 510 s respectively for ZnO sensor. The vertical alignment of ZnO nanorods as well as its surface modification by CuO nanoparticles increased the effective surface area of the device and the formation of *p*-CuO/*n*-ZnO junction at the interface are the reasons for the improved performance at room temperature. In addition to ethanol, the fabricated device has the capability to detect the presence of reducing gases like hydrogen sulfide and ammonia at room temperature.

Keywords: ZnO/CuO hierarchical structure, Hydrothermal, Room temperature gas detection, p–n Heterojunction

Introduction

The effective detection and removal of toxic gases in the atmosphere is important for human as well as any living organisms. The uncontrolled release of toxic gases such as CO, H_2S, NH_3, CH_3CH_2OH, etc. from automobiles, industries, laboratories, etc. cause severe health problems and they may even cause death [1–3]. The use of nanostructured materials for fabricating gas sensors with high sensitivity and selectivity is attracting attention of researchers nowadays because these materials can be easily synthesized and integrated into low cost portable gas detection devices [4, 5]. Among the various nanostructured materials, metal oxide nanostructures belong to the widely accepted category for fabricating gas sensors especially because of their chemical and thermal stability, tunable electrical and optical properties, etc. [6, 7].

Numerous metal oxide nanomaterials such as ZnO, TiO_2, SnO_2, WO_3 etc. [8–11] are commonly used in the field of gas sensing. Nanomaterials are already established in the field of gas sensing especially because of their high sensitivity originated due to their large surface to volume ratio [11]. One dimensional ZnO nanorods are attractive candidates for gas sensor applications because of their increased surface to volume ratio compared to other morphologies of ZnO and most importantly they provide an easy path way for electron transfer. There are several techniques such as doping, forming hierarchical structures, etc. which can be employed to improve the gas sensing properties especially to lower the operating temperature of metal oxide nanostructure based gas sensors. Among the various methods available, forming hierarchical structures using metals (Au, Ag, Pt, Pd, etc.) or metal oxides (CuO, Cu_2O, TiO_2, SnO_2, etc.) [12–14] is an effective way to enhance the various properties of metal oxide gas sensors. Researchers have already found the enhanced gas sensing characteristics of

*Correspondence: mkj@cusat.ac.in
Nanophotonic and Optoelectronic Devices Laboratory, Department of Physics, Cochin University of Science and Technology, Kochi 682022, Kerala, India

metal oxide/metal oxide hierarchical structures [15–17]. The hierarchical structure can form either p–n, n–n or p–p type semiconductor junctions depending on the nature of the material under consideration. In the present study we have investigated the enhanced gas sensing characteristics of *n*-ZnO/*p*-CuO hierarchical structures. Vertically aligned ZnO nanorods were grown by seed mediated hydrothermal method and CuO nanoparticles were loaded on the surface of ZnO nanorods via simple wet chemical method. ZnO is a well known n-type semiconductor having a direct band gap of 3.37 eV [18]. Various nanostructures of ZnO are used in several application such as photovoltaic [19], gas sensors [20], spintronics [21], etc. CuO is a p-type semiconducting material with a band gap of 1.35 eV which is widely being used in the fields of solar energy conversion [22], gas sensors [23], batteries [24], magnetic storage media [25], transparent electronics etc. *p*-CuO and *n*-ZnO can be combined in different ways to utilize the advantages of p-n heterojunction in gas sensor applications. The improvement in sensing performance of these composites have been attributed to many factors, including electronic effects [26] such as: band bending due to Fermi level equilibration, charge carrier separation, depletion layer manipulation and increased interfacial potential barrier energy. The chemical effects [27] such as decrease in activation energy, targeted catalytic activity and synergistic surface reactions; and geometrical effects [28] such as grain refinement, surface area enhancement, and increased gas accessibility also leads to the improvement in sensing. In addition to achieving better sensor characteristics, minimization of operating temperature and power consumption are the current trends in gas sensor technology. Most of the gas sensors based on metal oxides operate at temperatures above 150 °C which increase the power consumption of the gas sensor. Also the high temperature operation inhibits the use of sensors in explosive environments. In this context the development of room temperature gas sensors with enhanced gas sensing performance have significant importance in the gas sensor industry.

Here, we have grown vertically aligned ZnO nanorods on ITO/glass substrates by a seed mediated hydrothermal method. The growth of ZnO nanorods oriented along c-axial direction by seed mediated hydrothermal method have already reported in literature [29]. ZnO/CuO hierarchical structures were synthesized by depositing CuO nanoparticles on ZnO by a wet chemical method followed by annealing at 250 °C in air. The *n*-ZnO/*p*-CuO heterojunction device was used to detect ethanol, hydrogen sulfide and ammonia at room temperature (29 °C).

Experimental

Materials

All the reagents used were analytically pure and used without further purification. Zinc acetate dihydrate ($Zn(CH_3COO)_2{\cdot}2H_2O$), sodium hydroxide (NaOH) and copper acetate hydrate ($Cu(CO_2CH_3)_2H_2O$) were purchased from fisher scientific. Ammonia solution, isopropyl alcohol and ethanol were purchased from Merck Millipore. De ionized water was obtained from an ultra filter system. ITO/glass substrates were purchased from Sigma Aldrich (surface resistivity 15–25 Ω/sq). The substrates were cleaned by standard cleaning procedure.

Synthesis and characterization

A thin layer of ZnO seed layer was deposited by immersing the cleaned ITO/glass substrate in a solution containing zinc acetate (0.025 M) and sodium hydroxide (0.05 M) in 100 ml ethanol. The substrate was immersed in the solution for 5 min and the dipping process repeated for 8 times to obtain a uniform ZnO layer over a considerable area of the substrate. In between each dipping process the sample was kept at 80 °C on a hot plate. The annealing of the substrates at the optimized temperature 250 °C in air results in the formation of ZnO nanoparticles. The ITO/glass substrate with ZnO nanoparticle seed layer will act as a lattice matched substrate for the hydrothermal growth of aligned ZnO nanorods. The precursor solution for hydrothermal experiment was prepared by dissolving zinc acetate (0.1 M) and ammonia (25%) in 100 ml de-ionized water. The solution was transferred into a Teflon lined autoclave with the seed layer coated substrate immersed horizontally facing up and kept at 180 °C for 1 h in a laboratory oven. After hydrothermal experiment the samples were taken out and sonicated in iso propyl alcohol for few seconds to remove the unaligned nanorods lying over the vertically aligned nanorods. CuO nanoparticles were deposited by a wet chemical method. 0.05 M copper acetate solution was prepared in ethanol at room temperature and ZnO sample was immersed in the solution for 1 h. After deposition the sample was annealed at 250 °C for 2 h in air to form ZnO/CuO heterostructure.

The crystal phase and crystallinity of ZnO/CuO hierarchical structure was investigated by glancing angle X-ray diffraction taken using PANalytical X'pert PRO high resolution X-ray diffractometer (HRXRD) with CuKα (λ = 1.5418 Å). The detailed microstructure of the samples was analyzed using JEM2100 transmission electron microscopy (TEM) measurements. Raman spectra were recorded using Horiba Jobin–Yvon LABRAM HR Raman spectrometer excited with the 514 nm line of an Ar^+ laser. The surface morphology of the samples was analyzed using Carl Zeiss field emission scanning

electron microscopy (FESEM). The absorption spectra of the samples were recorded using JASCO V-570 spectrophotometer. Room temperature photoluminescence (PL) of the samples were measured using Horiba Jobin–Yvon Fluoromax-3 spectrofluorimeter using Xe lamp as the excitation source. The p–n junction characteristics of the device were studied using Keithley 4200 Semiconductor analyzer.

Gas sensors were fabricated by depositing circular gold electrodes on the top of the samples by thermal evaporation technique. The gas sensing measurements were done in a homemade stainless steel chamber by applying constant voltage. The applied voltage was 1 V for ZnO alone and 8 V for ZnO/CuO structure. Initially we measured the current through the sensor in synthetic air until it reaches a stable value. For all the sensing measurements commercially available high purity sample gases with moisture content less than 2 ppm have been used. Various concentrations of target gas have been injected into the chamber and the corresponding variation in the current through the sample was measured using Keithley source measure unit. After each measurement the chamber opened and samples have been exposed to air to attain the initial resistance. The response of the sensor can be defined as

$$S = \frac{I_g - I_a}{I_a} \quad (1)$$

where I_g and I_a are the current measured in the presence of the target gas and synthetic air respectively. We have taken I_a as the average value of first 50 points measured in the presence of air which is used for calculating the sensor parameters. The response time and recovery time of the sensor can be defined as the time taken for the sensor to reach 90% and 10% of the maximum response respectively.

Results and discussion

The crystal structure as well as crystallinity of the samples was analyzed using high resolution glancing angle X-ray diffraction shown in Fig. 1. The highly dispersed small CuO nanoparticles were not identified with X-ray diffraction. All the observed diffraction peaks correspond to wurtzite hexagonal ZnO and no peaks corresponding to CuO have been observed in the spectra. The high intensity of the peak along (0002) direction confirms the c-axial growth of ZnO nanorods [30].

The microstructure of the samples was further analyzed using TEM measurements. The TEM image in Fig. 2a shows the one dimensional morphology of the nanorods and the observed lattice planes in Fig. 2b matches with (0002) plane of ZnO with a lattice spacing of 2.6 Å. The CuO nanoparticles can be seen on the surface of ZnO

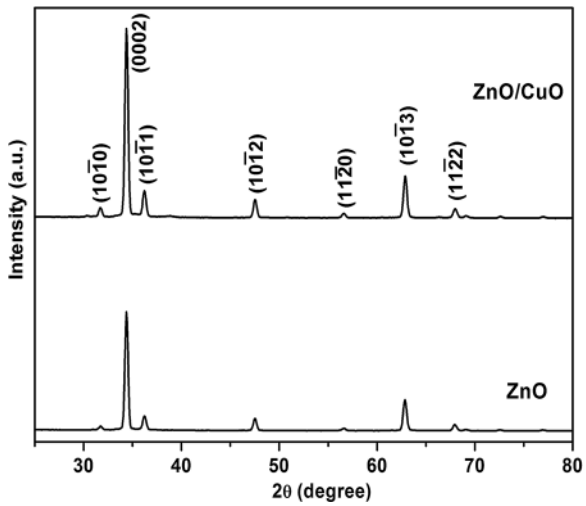

Fig. 1 Glancing angle X-ray diffraction pattern of ZnO and ZnO/CuO hierarchical structure

nanorods in Fig. 2c which make the nanorod surface rough. The presence of bright spots in the SAED pattern in Fig. 2d indicates the crystalline nature of ZnO/CuO structure [30]. In addition to (0002), $(10\bar{1}0)$ and $(10\bar{1}1)$ planes of wurtzite hexagonal ZnO, $(\bar{1}11)$ lattice plane of monoclinic CuO can also be observed in the SAED pattern confirming the formation of ZnO/CuO hierarchical structures.

Micro Raman spectroscopy is a non destructive technique used for analyzing the vibrational properties of materials. The Raman spectra of both ZnO and ZnO/CuO are displayed in Fig. 3. All the observed vibrational modes such as E_{2L} (98 cm^{-1}), $A1_{TO}$ (381 cm^{-1}), E_{2H} (437 cm^{-1}), and $E1_{LO}$ (580 cm^{-1}) corresponds to wurtzite hexagonal structure of ZnO. Monoclinic CuO exhibit three Raman active modes (Ag + 2Bg) which are assigned respectively at 278 cm^{-1} (A_g), 333 cm^{-1} (B_{1g}) and 620 cm^{-1} (B_{2g}) [31, 32]. Along with the vibrations of ZnO, A_g mode corresponding to monoclinic CuO has been observed for ZnO/CuO heterostructure. The Raman vibrations of CuO are highly dependent on the method of preparation and this may be the reason for the absence of B_{2g} vibration. The co-existence of ZnO and CuO Raman modes in the Raman spectra confirms the formation of ZnO/CuO hierarchical structure.

The surface morphology of all the samples was analyzed using FESEM images depicted in Fig. 4. The vertical alignment of nanorods against the substrate surface forms a porous network which makes the gas diffusion in and out easier [30]. The sonication has effectively removed the unaligned nanorods lying over the vertically aligned nanorods shown in the inset of Fig. 4a. The diameter and length of the nanorods are approximately 95 nm

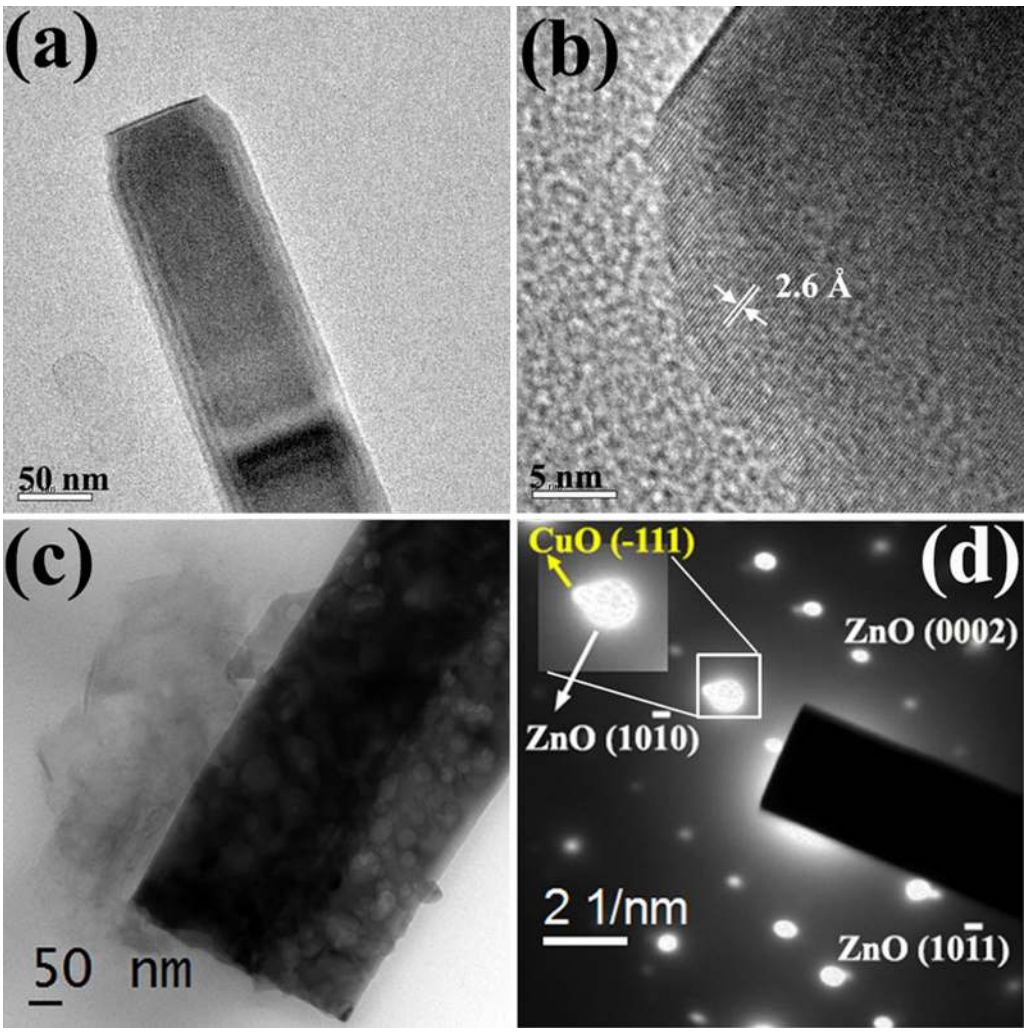

Fig. 2 **a** TEM and **b** HRTEM images of ZnO nanorod, **c** TEM image and **d** SAED pattern of ZnO/CuO hierarchical structure

and 2 μm respectively. The presence of CuO on ZnO nanorods can be clearly seen in Fig. 4d. The attachment of CuO increases the interfacial area and correspondingly an enhanced gas sensing behavior can be observed.

The UV–visible absorption spectra of ZnO and ZnO/CuO hierarchical structures are shown in Fig. 5. The spectra of pure ZnO nanorods possess an absorption at around 370 nm corresponding to the band gap of ZnO whereas the band gap absorption edge get slightly red shifted to 374 nm in the case of ZnO/CuO hierarchical structure similar to that observed in previous reports [33, 34]. Also the ZnO/CuO sample has a high value of absorbance in the visible region compared to pristine ZnO. These factors confirm the formation of CuO loaded ZnO hierarchical structures.

The defects such as oxygen vacancies, zinc interstitials, etc. in ZnO nanostructures affects the electronic and surface properties of the semiconductor [35, 36]. The presence of these defect states are in correlation with the performance of a semiconductor gas sensor. Photoluminescence (PL) is a non destructive technique to analyze the defect states in materials. The room temperature PL emission spectra of ZnO and ZnO/CuO heterostructures excited at 325 nm are shown in Fig. 6. For both the samples emissions bands are observed in the UV as well as in the visible region of the electromagnetic spectrum. The UV emission shoulder at 378 nm corresponds to the characteristic emission closely related to the band gap of ZnO. The emission bands in the visible region can be attributed to the transitions between various defect levels within the band gap of ZnO [37, 38]. Oxygen vacancies are one of the important defect states especially in metal oxides which make most of them n-type semiconductors. The emission band at 564 nm in both ZnO and ZnO/

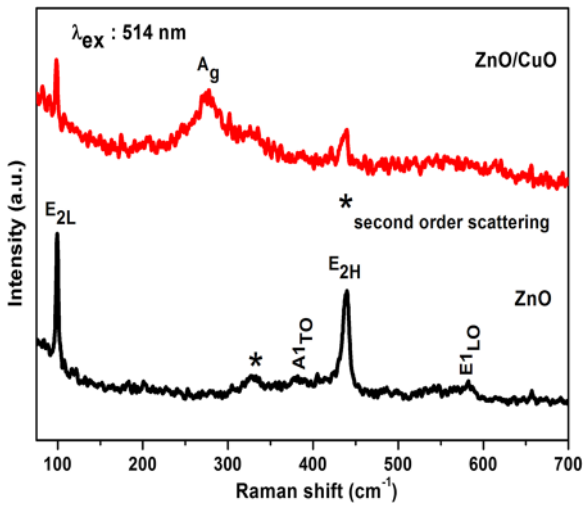

Fig. 3 Micro Raman spectra of ZnO and ZnO/CuO hierarchical structure

CuO samples corresponds to the presence of oxygen vacancies which make them suitable for the fabrication of gas sensors [39] because gas sensing is solely a surface phenomenon which depends mainly on the exposed surface area and the presence of oxygen vacancies in the sensing material. Thus both Raman and PL confirm the presence of considerable amount of oxygen vacancies in ZnO and ZnO/CuO structures. The intensity of defect related emissions got reduced in ZnO/CuO which can be attributed to the formation of *p*-CuO/*n*-ZnO junctions suppressing the recombination of carriers. The increased intensity of band edge emission in ZnO/CuO is due to the annealing of the sample at 250 °C.

The room temperature (29 °C) ethanol sensing characteristics of ZnO and ZnO/CuO nanostructures were monitored by measuring the change in current upon exposure to different concentrations of the target gas. The response of ZnO and ZnO/CuO to various concentrations of ethanol is shown in Fig. 7. The room

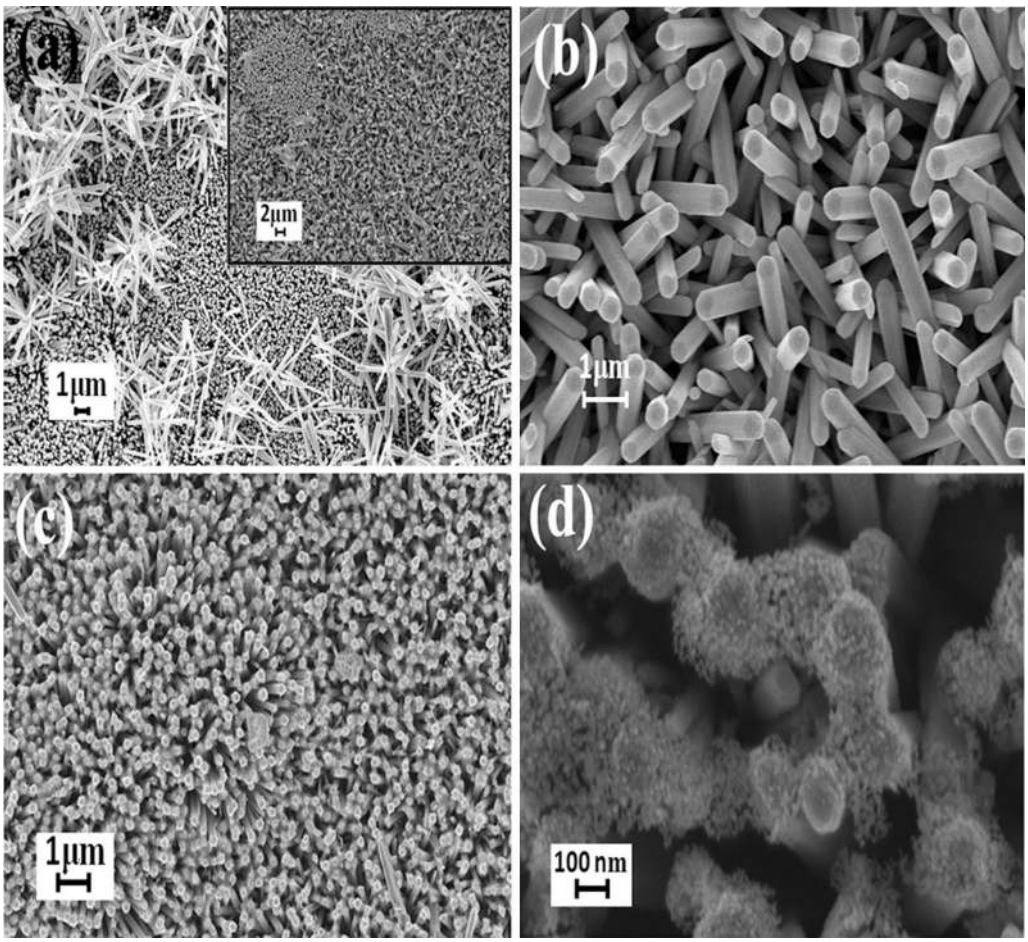

Fig. 4 FESEM images of **a** as grown ZnO nanorods (inset shows the image of sonicated sample), **b** magnified view of the sonicated sample, **c** CuO attached ZnO nanorods and **d** magnified view of ZnO/CuO

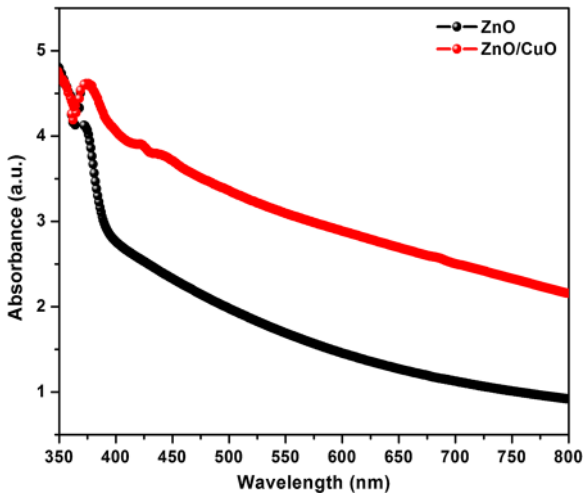

Fig. 5 UV–visible absorption spectra of ZnO and ZnO/CuO structures

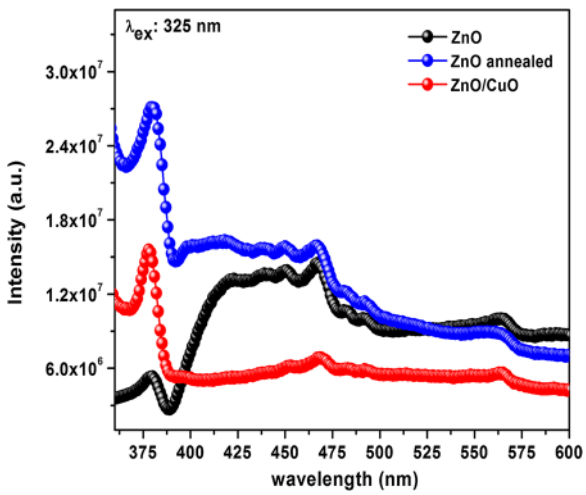

Fig. 6 Photoluminescence emission spectra of ZnO and ZnO/CuO heterostructures

temperature response of the sensor increases in ethanol ambient due to the redox reactions taking place between the metal oxide and the target gas which will be discussed later. The room temperature (29 °C) operation of the sensor prevents the grain growth in the sensing material and also reduces the power consumption of the device. Both ZnO and ZnO/CuO samples exhibit very good response to ethanol even for 5 ppm concentration at room temperature. The response of both the sensors increases with increase in concentration of the target gas. Compared to pristine ZnO, ZnO/CuO exhibit improved response values for all the concentrations used in the present study. The vertical alignment as well as the attachment of CuO nanoparticles on ZnO nanorod surface increases the exposed surface area of the sensor contributing to the enhanced sensing characteristics. More importantly the p–n junctions formed at the interface of *n*-ZnO and *p*-CuO significantly improve the gas sensor performance. The detailed mechanism of the heterojunction device will be discussed later.

Figure 8 shows that the response of ZnO/CuO structure is higher than the response of ZnO for all target gas concentrations. The response and recovery time of the fabricated sensors are depicted in Fig. 9. It can be seen that the response time decreases with increase in concentration whereas the recovery time increases with increase in target gas concentration. This can be attributed to the number of molecules having minimum required energy for the reaction increases at high concentrations hence more and more target gas molecules react with adsorbed oxygen ions resulting in faster change in resistance. Whereas the adsorption takes place slowly at low concentrations due to the lower coverage of gas molecules hence the change in resistance also takes place slowly. The significance of the present work is that even at room temperature both the sensors respond to 5 ppm ethanol gas within less than 100 s. The response time calculated is 98 and 30 s for ZnO and ZnO/CuO respectively and almost complete desorption of the target gas takes place especially at lower concentrations within a few minutes. A good sensor should have high value of response and low value of response time. The complete solution processed p-n heterojunction sensor fabricated in the present study exhibit very good values of gas sensor parameters at room temperature compared to the previous reports [40, 41]. The high value of recovery time of the devices is due to the slow desorption rate of ethanol at room temperature [42]. The incorporation of suitable noble metal additives such as Ag, Au, Pd, Pt, etc. is an effective way to improve the response time of metal oxide based gas sensors [43, 44].

The selectivity of ZnO/CuO nanostructure has been studied by testing the response of the device to different types of target gases. Figure 10 shows the response of ZnO/CuO sensor to 40 ppm concentration of ethanol, hydrogen sulfide and ammonia. The response value is 5.08 for ethanol whereas it is 2.091 and 0.772 for hydrogen sulfide and ammonia respectively indicating good selectivity towards ethanol. This is because the electron donating effect of different types of gas molecules is different which depends on the nature of the gas as well as the sensor material.

Table 1 compares the gas sensing characteristics of ZnO/CuO gas sensor with the present work. The simple processing technique and better gas sensing parameters make the fabricated device in the present work a

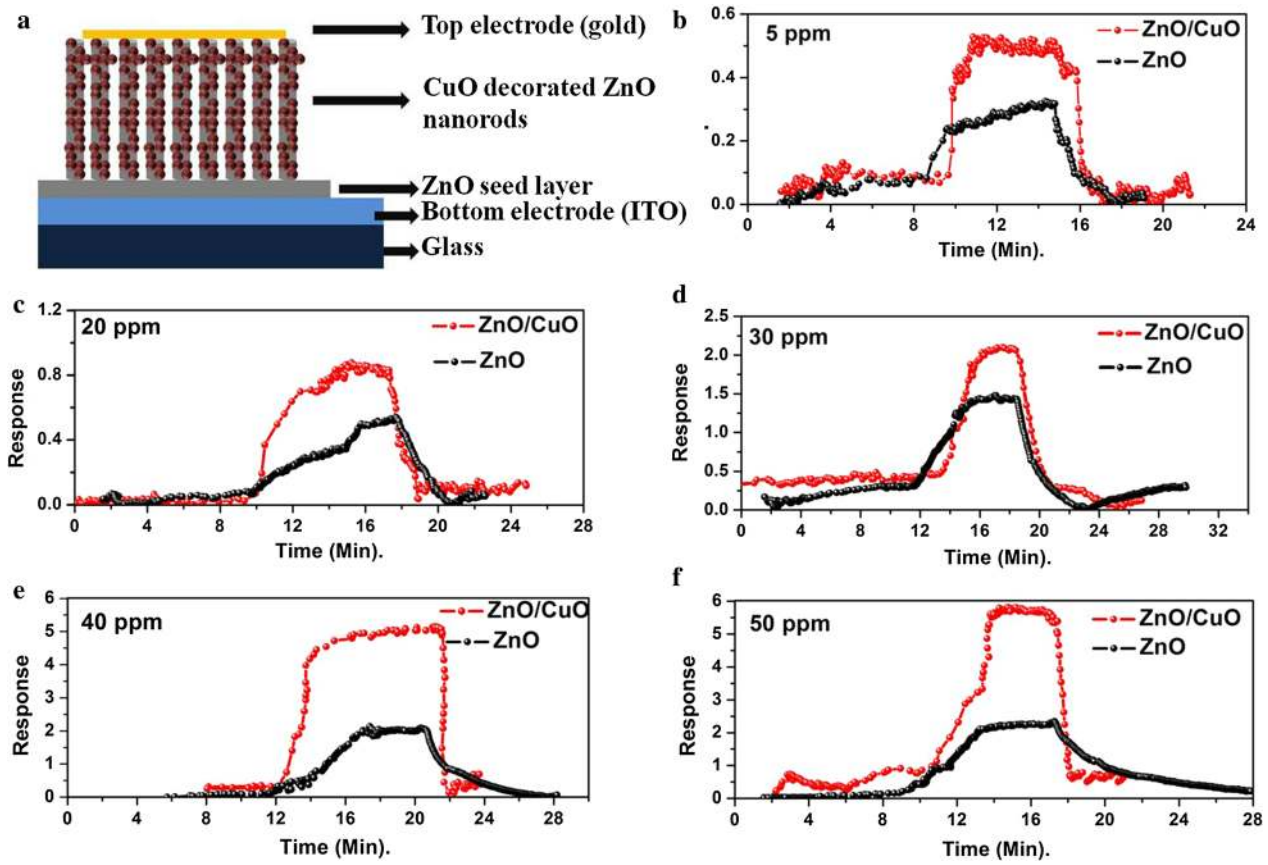

Fig. 7 Schematic representation of the **a** device structure and **b**–**f** room temperature ethanol sensing characteristics of ZnO and ZnO/CuO nanostructures

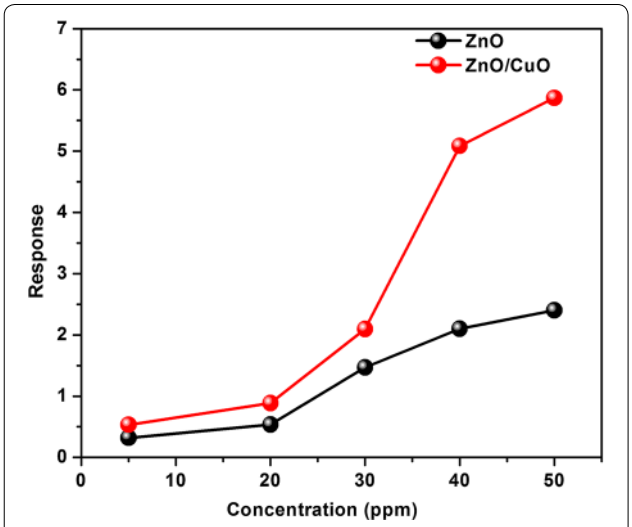

Fig. 8 Comparison of ethanol response of ZnO and ZnO/CuO structures

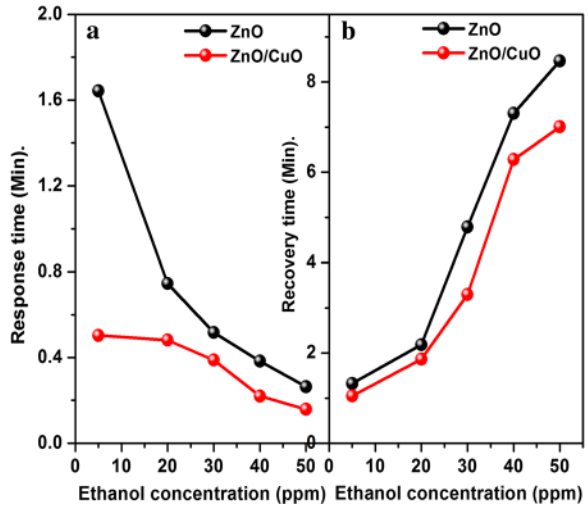

Fig. 9 **a** Response and **b** recovery time of ZnO and ZnO/CuO structures to ethanol

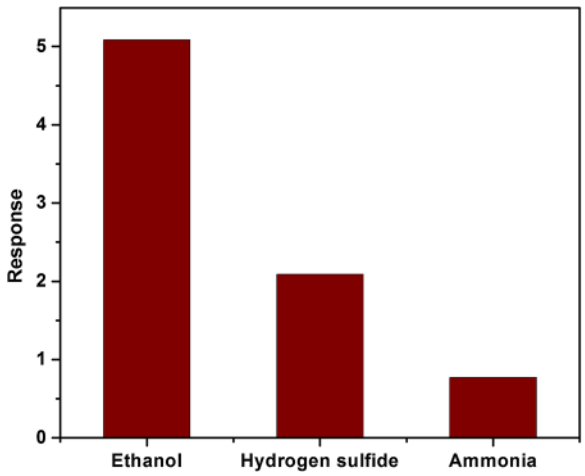

Fig. 10 Response of ZnO/CuO hierarchical structure to various reducing gases (40 ppm) at room temperature

promising candidate for the development of room temperature gas sensors.

CuO hierarchical structure exhibit good response to various reducing gases and the fabricated devices are more selective to ethanol at room temperature (29 °C). The basic gas sensing mechanism of metal oxide semiconductors relies on the interaction between the adsorbed oxygen molecules on the surface of the sensor material and the target gas [5, 7, 48–51]. Generally O_2^- at temperature < 100 °C and O^- and O^{2-} at temperature > 100 °C are the dominant oxygen species adsorbed on the semiconductor. The adsorption of oxygen ions on the surface of oxide semiconductor forms an electron depletion region by withdrawing electrons from the conduction band. The interaction between the adsorbed oxygen ions and ethanol gas release electrons back to the semiconductor consequently the depletion layer width and resistance of the semiconductor decreases.

The reasons for the improved sensing behavior of ZnO/CuO hierarchical structures can be attributed to 1) increased number of active sites for gas adsorption [52] and 2) the formation of p-n heterojunctions at the interface of *p*-CuO and *n*-ZnO [15, 53, 54]. The high surface to volume ratio of nanorods and the presence of CuO nanoparticles together increased the number of gas adsorption sites. Also the nanogaps in the nanorod array make more target gas molecules to penetrate into the sensing material. The schematic energy band diagram of *p*-CuO/*n*-ZnO heterojunction at thermal equilibrium is shown in Fig. 11b. Generally oxygen deficient ZnO exhibit n-type and oxygen excess CuO exhibit p-type conductivity. When there is a difference in Fermi energy between the materials forming a junction, electrons from the higher energy will flow across the interface to the lower energy until the Fermi energies have equilibrated. This leads to the formation of a depletion region and a potential barrier at the interface. The presence of a number of p–n junctions at the interface results in a remarkable increase in the resistance of the heterostructure compared to pristine ZnO or CuO. The total resistance of the heterostructure will be contributed by the depletion layer on ZnO, accumulation layer on CuO and the depletion region at the junction and the increased resistance is clear from the current–voltage (I–V) characteristics in Fig. 12. Because of this increased resistance of the heterojunction we have chosen a voltage (8 V) higher than the turn on voltage of the diode for sensing measurements. The response time and recovery time of the sensor depends on the activation energy for gas adsorption and desorption and rate of gas desorption. Both these factors depend on the morphology and composition of the sensing material. In the present work the one dimensional morphology of ZnO as well as the attachment of CuO nanoparticles increase the number of adsorption sites for oxygen and may decrease the activation energy for gas adsorption and desorption

Table 1 Evaluation of the development of gas sensors based on ZnO/CuO structures

Method of synthesis	Sensor working temperature (°C)	Target gas concentration (ppm)	Response	Response time (s)	Recovery time (s)	References
Hydrothermal	220	Ethanol 100	25.5[a]	6	42	[45]
Hydrothermal	300	Ethanol 100	98.8[b]	7	9	[46]
Solid state reaction	Room temperature	Ethanol 150	2.3[b]	70	88	[41]
Pulsed laser deposition	Room temperature	Hydrogen sulphide 15	78[c]	180	15	[47]
Hydrothermal	Room temperature	Ethanol 5	0.53[d]	30	63	Present work
		50	5.87[d]	9	420	

[a] $S = \frac{V_g(5000\,mV - V_a)}{V_a(5000\,mV - V_g)}$

[b] $S = \frac{R_a}{R_g}$

[c] $S = \left(\frac{I_g - I_a}{I_a}\right) \times 100$

[d] $S = \left(\frac{I_g - I_a}{I_a}\right)$

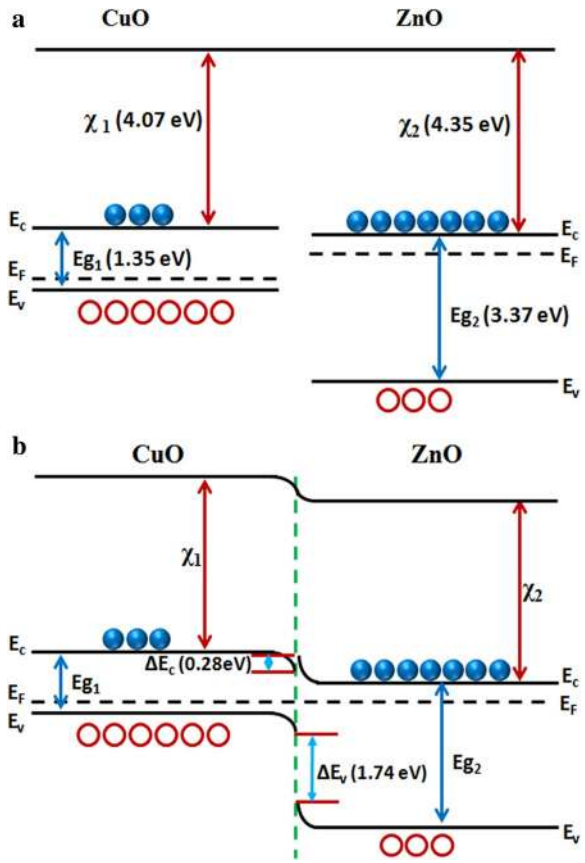

Fig. 11 Energy-band diagram of **a** CuO and ZnO and **b** ZnO/CuO heterojunction device at thermal equilibrium

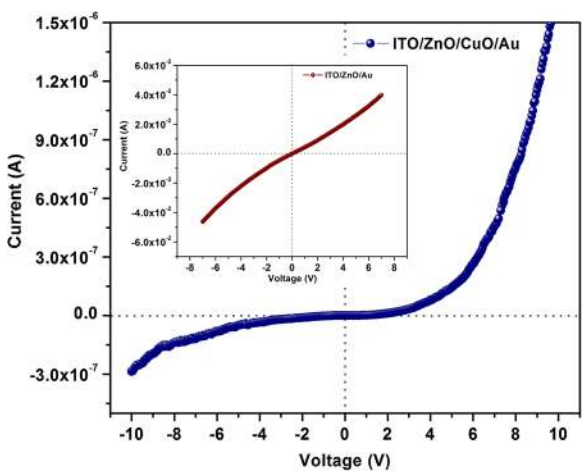

Fig. 12 Current–voltage characteristics of ZnO/CuO hierarchical structure (Inset shows the I–V characteristics of ZnO alone

processes at room temperature resulting in enhanced gas sensing performance.

In the energy band diagram shown in Fig. 11, E_{g1} (1.35 eV), χ_1 (4.07 eV) and E_{g2} (3.37 eV), χ_2 (4.35 eV) represents band gaps and electron affinities [16, 23, 46, 55] of CuO and ZnO respectively. The barrier height of conduction band ($\Delta E_C = \chi_2 - \chi_1$) and valence band $\left[\Delta E_V = \left(E_{g2} - E_{g1}\right) - \Delta E_C\right]$ at the p–n junction were 0.28 eV and 1.74 eV respectively. The generated free electrons on adsorption of ethanol gas in ZnO can easily transport through the p–n junction due to the low value of ΔE_C and at the same time the holes in CuO will accumulate at the valence band of p–CuO due to the large value of ΔE_V. At low temperatures the dissociation of ethanol into aldehyde (CH_3CHO) and H_2O are prominent than the formation of CO_2 and H_2O [41, 56, 57]. At room temperature the dehydrogenation of ethanol molecules generate OH^- ions (breaking of C-O bond) and $[CH_3CH_2O]^-$ ions (breaking of O–H bond) due to the lower bond breaking energy of C-O and O–H bonds. Ethanol vapor can be easily attached to metal oxide surfaces in the form of dehydrogenated ionic fragment $[CH_3CH_2O]^-$ through the interaction of adsorbed oxygen on metal oxide surfaces represented by the Eq. (2). Also at the interface of ZnO/CuO junction ethanol molecules react with holes in CuO [51, 58–60] followed by the Eq. (3).

$$CH_3CH_2OH_{(g)} + O^-_{2(ads)} \rightarrow \begin{cases} [CH_3CH_2O]^-_{(ads)} + OH^-_{(ads)} \\ CH_3CHO + H_2O + e^- \end{cases} \quad (2)$$

$$CH_3CH_2OH_{(g)} + 2h^+ + e^- + O^-_{2(ads)} \rightarrow CH_3CHO + H_2O + e^- \quad (3)$$

These reactions release free electrons resulting in the enhanced room temperature gas sensing performance of *p*-CuO/*n*-ZnO heterojunction device.

Conclusions

ZnO/CuO heterojunction gas sensor has been successfully fabricated by low temperature solution processing and its room temperature (29 °C) response to various reducing gases has been investigated. Working at room temperature, the response to ethanol gas of the fabricated device is higher than to hydrogen sulfide or ammonia gases. All the gas sensor parameters have been improved by the incorporation of CuO nanoparticles on ZnO nanorods. The easy preparation technique

and room temperature gas sensing of the samples will make the practical use of these devices with reduced power consumption a reality.

Authors' contributions

PPS has made significant contribution in the preparation and characterizations of samples, collected data, analyzed and wrote the manuscript. MKJ has revised the manuscript for intellectual content and corrected accordingly. Both authors read and approved the final manuscript.

Acknowledgements

The work was supported by Nanomission council (DST NO. SR/NM/NS-22/2008), Department of Science and Technology, India. Author PPS thanks the University Grant Commission (UGC) for research fellowship.

Competing interests

The authors declare that they have no competing interests.

Publisher's Note

Received: 28 August 2017 Accepted: 16 January 2019
Published online: 29 January 2019

References

1. Azad AM, Akbar SA, Mhaisalkar SG et al (1992) Solid-state gas sensors: a review. J Electrochem Soc 139:3690–3704. https://doi.org/10.1149/1.2069145
2. Bogue RW (1996) Handbook of chemical and biological sensors. Meas Sci Technol 1:1. https://doi.org/10.1088/0957-0233/7/9/018
3. Wu Y-R, Singh J (2004) Metal piezoelectric semiconductor field effect transistors for piezoelectric strain sensors. Appl Phys Lett 85:1223–1225. https://doi.org/10.1063/1.1784039
4. Kolmakov A, Moskovits M (2004) Chemical sensing and catalysis by one-dimensional metal-oxide nanostructures. Annu Rev Mater Res 34:151–180. https://doi.org/10.1146/annurev.matsci.34.040203.112141
5. Comini E, Baratto C, Concina I et al (2013) Metal oxide nanoscience and nanotechnology for chemical sensors. Sens Actuators B Chem 179:3–20. https://doi.org/10.1016/j.snb.2012.10.027
6. Zhang J, Qin Z, Zeng D, Xie C (2017) Metal-oxide-semiconductor based gas sensors:screening, preparation, and integration. Phys Chem Chem Phys 19:6313–6329. https://doi.org/10.1039/c6cp07799d
7. Sun Y-F, Liu S-B, Meng F-L et al (2012) Metal oxide nanostructures and their gas sensing properties: a review. Sensors 12:2610–2631. https://doi.org/10.3390/s120302610
8. Gurav KV, Gang MG, Shin SW et al (2014) Gas sensing properties of hydrothermally grown ZnO nanorods with different aspect ratios. Sens Actuators B Chem 190:439–445. https://doi.org/10.1016/j.snb.2013.08.069
9. Wang JX, Sun XW, Yang Y et al (2006) Hydrothermally grown oriented ZnO nanorod arrays for gas sensing applications. Nanotechnology 17:4995–4998. https://doi.org/10.1088/0957-4484/17/19/037
10. Barsan N, Weimar U (2003) Understanding the fundamental principles of metal oxide based gas sensors; the example of CO sensing with SnO_2 sensors in the presence of humidity. J Phys 15:R813–R839. https://doi.org/10.1088/0953-8984/15/20/201
11. Korotcenkov G (2007) Metal oxides for solid-state gas sensors: what determines our choice? Mater Sci Eng B 139:1–23. https://doi.org/10.1016/j.mseb.2007.01.044
12. Zainelabdin A, Amin G, Zaman S et al (2012) CuO/ZnO Nanocorals synthesis via hydrothermal technique: growth mechanism and their application as Humidity Sensor. J Mater Chem 22:11583–11590. https://doi.org/10.1039/c2jm16597j
13. Guo Z, Chen X, Li J et al (2011) ZnO/CuO hetero-hierarchical nanotrees array: hydrothermal preparation and self-cleaning properties. Langmuir 27:6193–6200. https://doi.org/10.1021/la104979x
14. Ding J, Zhu J, Yao P et al (2015) Synthesis of ZnO–Ag hybrids and their gas-sensing performance toward ethanol. Ind Eng Chem Res 54:8947–8953. https://doi.org/10.1021/acs.iecr.5b01711
15. Miller DR, Akbar SA, Morris PA (2014) Nanoscale metal oxide-based heterojunctions for gas sensing: a review. Sens Actuators B Chem 204:250–272. https://doi.org/10.1016/j.snb.2014.07.074
16. Zainelabdin A, Zaman S, Amin G et al (2012) Optical and current transport properties of CuO/ZnO nanocoral *p–n* heterostructure hydrothermally synthesized at low temperature. Appl Phys A 108:921–928. https://doi.org/10.1007/s00339-012-6995-2
17. Xu H, Ju J, Li W et al (2016) Superior triethylamine-sensing properties based on TiO_2/SnO_2 *n–n* heterojunction nanosheets directly grown on ceramic tubes. Sens Actuators B Chem 228:634–642. https://doi.org/10.1016/j.snb.2016.01.059
18. Özgür Ü, Alivov YI, Liu C et al (2005) A comprehensive review of ZnO materials and devices. J Appl Phys 98:1–103. https://doi.org/10.1063/1.1992666
19. Huang J, Yin Z, Zheng Q (2011) Applications of ZnO in organic and hybrid solar cells. Energy Environ Sci 4:3861–3877. https://doi.org/10.1039/C1EE01873F
20. Galstyan V, Comini E, Ponzoni A et al (2016) ZnO Quasi-1D nanostructures: synthesis, modeling, and properties for applications in conductometric chemical sensors. Chemosensors 4:1–21. https://doi.org/10.3390/chemosensors4020006
21. Pan F, Song C, Liu XJ et al (2008) Ferromagnetism and possible application in spintronics of transition-metal-doped ZnO films. Mater Sci Eng R 62:1–35. https://doi.org/10.1016/j.mser.2008.04.002
22. Yu Y-Y, Chien W-C, Wang Y-J (2016) Copper oxide hole transport materials for heterojunction solar cell applications. Thin Solid Films 618:1–7. https://doi.org/10.1016/j.tsf.2016.04.001
23. Wang C, Fu XQ, Xue XY et al (2007) Surface accumulation conduction controlled sensing characteristic of p-type CuO nanorods induced by oxygen adsorption. Nanotechnology 18:145506. https://doi.org/10.1088/0957-4484/18/14/145506
24. Su D, Xie X, Dou S, Wang G (2014) CuO single crystal with exposed 001 facets–a highly efficient material for gas sensing and Li-ion battery applications. Sci Rep 4:5753. https://doi.org/10.1038/srep05753
25. Dar MA, Kim YS, Kim WB et al (2008) Structural and magnetic properties of CuO nanoneedles synthesized by hydrothermal method. Appl Surf Sci 254:7477–7481. https://doi.org/10.1016/j.apsusc.2008.06.004
26. Mario B, Niederberger M (2017) The role of interfaces in heterostructures. ChemPlusChem 82:42–59. https://doi.org/10.1002/cplu.201600519
27. Wang C, Yin L, Zhang L et al (2010) Metal oxide gas sensors: sensitivity and influencing factors. Sensors. https://doi.org/10.3390/s100302088
28. Liangyuan C, Shouli B, Guojun Z et al (2008) Synthesis of ZnO–SnO_2 nanocomposites by microemulsion and sensing properties for NO2. Sens Actuators B Chem 134:370–376. https://doi.org/10.1016/j.snb.2008.04.040
29. Lee Y-J, Sounart TL, Scrymgeour DA et al (2007) Control of ZnO nanorod array alignment synthesized via seeded solution growth. J Cryst Growth 304:80–85. https://doi.org/10.1016/j.jcrysgro.2007.02.011
30. Xu Q, Ju D, Zhang Z et al (2016) Near room-temperature triethylamine sensor constructed with CuO/ZnO P–N heterostructural nanorods directly on flat electrode. Sensors Actuators B Chem 225:16–23. https://doi.org/10.1016/j.snb.2015.10.108
31. Wang JX, Sun XW, Yang Y et al (2011) Free-standing ZnO–CuO composite nanowire array films and their gas sensing. Nanotechnology 22:325704. https://doi.org/10.1088/0957-4484/22/32/325704
32. Zhu BY, Sow C-H, Yu T et al (2006) Co-synthesis of ZnO–CuO nanostructures by directly heating brass in air. Adv Funct Mater 16:2415–2422. https://doi.org/10.1002/adfm.200600251
33. Vuong NM, Chinh ND, Huy BT, Lee Y (2016) CuO-decorated ZnO hierarchical nanostructures as efficient and established sensing materials for H_2S gas sensors. Sci Rep 6:26736. https://doi.org/10.1038/srep26736
34. Qamar MT, Aslam M, Ismail IMI et al (2015) Synthesis, characterization, and sunlight mediated photocatalytic activity of CuO coated ZnO for the removal of nitrophenols. ACS Appl Mater Interfaces 7:8757–8769. https://doi.org/10.1021/acsami.5b01273
35. Lupan O, Ursaki VV, Chai G et al (2010) Selective hydrogen gas nanosensor using individual ZnO nanowire with fast response at room temperature. Sensors Actuators B Chem 144:56–66. https://doi.org/10.1016/j.snb.2009.10.038

36. Zhang Y, Xu J, Xiang Q et al (2009) Brush-Like Hierarchical ZnO nanostructures: synthesis, photoluminescence and gas sensor properties. J Phys Chem C 113(9):3430–3435. https://doi.org/10.1021/jp8092258
37. Meyer BK, Alves H, Hofmann DM et al (2004) Bound exciton and donor-acceptor pair recombinations in ZnO. Phys Status Solidi Basic Res 241:231–260. https://doi.org/10.1002/pssb.200301962
38. Zeng H, Duan G, Li Y et al (2010) Blue luminescence of ZnO nanoparticles based on non-equilibrium processes: defect origins and emission controls. Adv Funct Mater 20:561–572. https://doi.org/10.1002/adfm.200901884
39. Ghosh M, Ningthoujam RS, Vatsa RK et al (2011) Role of ambient air on photoluminescence and electrical conductivity of assembly of ZnO nanoparticles. J Appl Phys 110:54309–1–54309–7. https://doi.org/10.1063/1.3632059
40. Shao C, Chang Y, Long Y (2014) High performance of nanostructured ZnO film gas sensor at room temperature. Sens Actuators B Chem 204:666–672. https://doi.org/10.1016/j.snb.2014.08.003
41. Yu MR, Suyambrakasam G, Wu RJ, Chavali M (2012) Performance evaluation of ZnO–CuO hetero junction solid state room temperature ethanol sensor. Mater Res Bull 47:1713–1718. https://doi.org/10.1016/j.materresbull.2012.03.046
42. Batzill M (2006) Surface science studies of gas sensing materials: Sno_2. Sensors 6:1345–1366. https://doi.org/10.3390/s6101345
43. Subha PP, Hasna K, Jayaraj MK (2017) Surface modification of TiO 2 nanorod arrays by Ag nanoparticles and its enhanced room temperature ethanol sensing properties Surface modification of TiO_2 nanorod arrays by Ag nanoparticles and its enhanced room temperature ethanol sensing properties. Mater Res Express 4:105037–105047. https://doi.org/10.1088/2053-1591/aa91ee
44. Yamazoe N, Kurokawa Y, Seiyama T (1983) The effects of additives on semiconductors. Sensors Actuators 4:283–289. https://doi.org/10.1016/0250-6874(83)85034-3
45. Huang J, Dai Y, Gu C et al (2013) Preparation of porous flower-like CuO/ZnO nanostructures and analysis of their gas-sensing property. J Alloys Compd 575:115–122. https://doi.org/10.1016/j.jallcom.2013.04.094
46. Bin Zhang Y, Yin J, Li L et al (2014) Enhanced ethanol gas-sensing properties of flower-like *p*-CuO/*n*-ZnO heterojunction nanorods. Sensors Actuators B Chem 202:500–507. https://doi.org/10.1016/j.snb.2014.05.111
47. Liu X, Du B, Sun Y et al (2016) Sensitive room temperature photoluminescence-based sensing of H_2S with novel CuO–ZnO nanorods. ACS Appl Mater Interfaces 8:16379–16385. https://doi.org/10.1021/acsami.6b02455
48. Shankar P, Bosco J, Rayappan B (2015) Gas sensing mechanism of metal oxides: the role of ambient atmosphere, type of semiconductor and gases—a review. Sci Lett J 4(126):1–18
49. Barsan N, Weimar UDO (2001) Conduction model of metal oxide gas sensors. J Electroceramics 7:143–167. https://doi.org/10.1023/A:1014405811371
50. Yamazoe N, Shimanoe K (2009) Receptor function and response of semiconductor gas sensor. J Sensors 2009:1–21. https://doi.org/10.1155/2009/875704
51. Acharyya D, Bhattacharyya P (2016) Alcohol sensing performance of ZnO hexagonal nanotubes at low temperatures: a qualitative understanding. Sens Actuators B Chem 228:373–386. https://doi.org/10.1016/j.snb.2016.01.035
52. Bin Zhang Y, Yin J, Li L et al (2014) Enhanced ethanol gas-sensing properties of flower-like *p*-CuO/*n*-ZnO heterojunction nanorods. Sens Actuators B Chem 202:500–507. https://doi.org/10.1016/j.snb.2014.05.111
53. Li T, Zeng W, Wang Z (2015) Quasi-one-dimensional metal-oxide-based heterostructural gas-sensing materials: a review. Sens Actuators B Chem 221:1570–1585. https://doi.org/10.1016/j.snb.2015.08.003
54. Guo Y, Gong M, Li Y et al (2016) Sensitive, selective, and fast detection of ppb-level H_2S gas boosted by ZnO–CuO mesocrystal. Nanoscale Res Lett 11(475):1–9. https://doi.org/10.1186/s11671-016-1688-y
55. Park S, Ko H, Kim S, Lee C (2014) Role of the Interfaces in Multiple Networked One-Dimensional Core-Shell Nanostructured Gas Sensors. ACS Appl Mater Interfaces 6:9595–9600. https://doi.org/10.1021/am501975v
56. Hazra A, Dutta K, Bhowmik B, Bhattacharyya P (2015) Highly repeatable low-ppm ethanol sensing characteristics of *p*-TiO_2-based resistive devices. IEEE Sens J 15:408–416. https://doi.org/10.1109/JSEN.2014.2345575
57. Song W, Liu P, Hensen EJM (2014) A mechanism of gas-phase alcohol oxidation at the interface of Au nanoparticles and a $MgCuCr_2O_4$ spinel support. Catal Sci Techol 4:2997–3003. https://doi.org/10.1039/c4cy00462k
58. Mendoza F, Hernández DM, Makarov V et al (2014) Room temperature gas sensor based on tin dioxide-carbon nanotubes composite films. Sens Actuators B Chem 190:227–233. https://doi.org/10.1016/j.snb.2013.08.050
59. Chen Y, Yu L, Feng D et al (2012) Superior ethanol-sensing properties based on Ni-doped SnO_2 p–n heterojunction hollow spheres. Sens Actuators B Chem 166–167:61–67. https://doi.org/10.1016/j.snb.2011.12.018
60. Chen YJ, Zhu CL, Xiao G (2008) Ethanol sensing characteristics of ambient temperature sonochemically synthesized ZnO nanotubes. Sens Actuators B 129:639–642. https://doi.org/10.1016/j.snb.2007.09.010